Surveying the Potential Energy Landscape of Monolayers on Surfaces

Energy Landscapes

Telluride, CO, 2007

Alexandre Tkatchenko

Chemistry Department, UAM-Iztapalapa, Mexico

sanix@ixil.izt.uam.mx

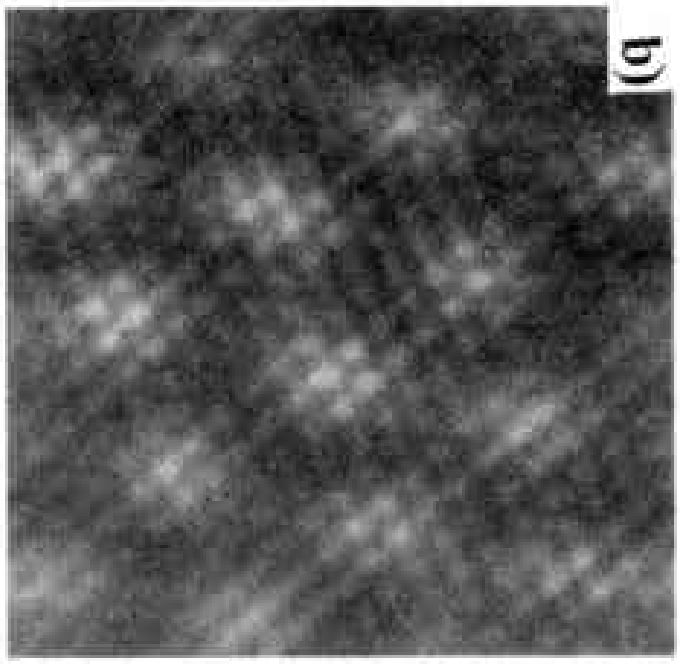

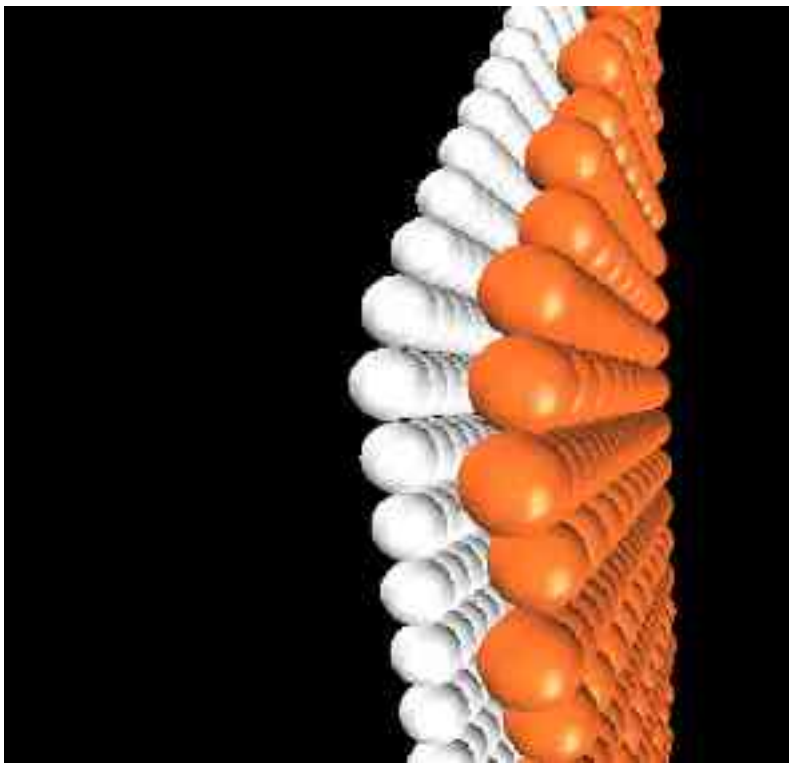

Rot-Hex. I-Au(111)

(√19x√19)-13-Co-Pt(111)

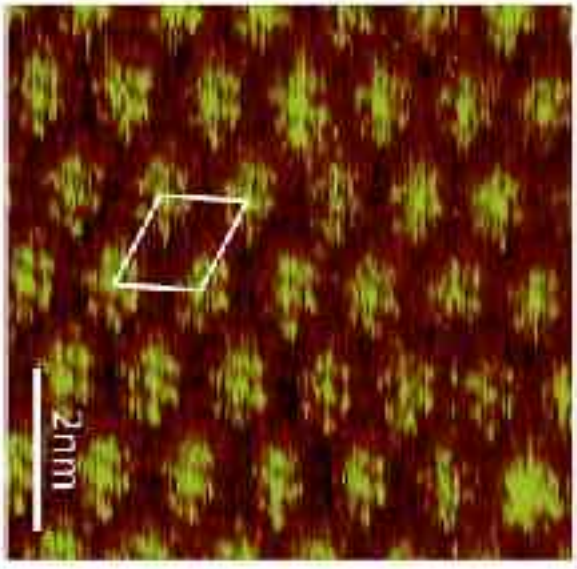

(√7x√7)R19.1. I-Pt(111)

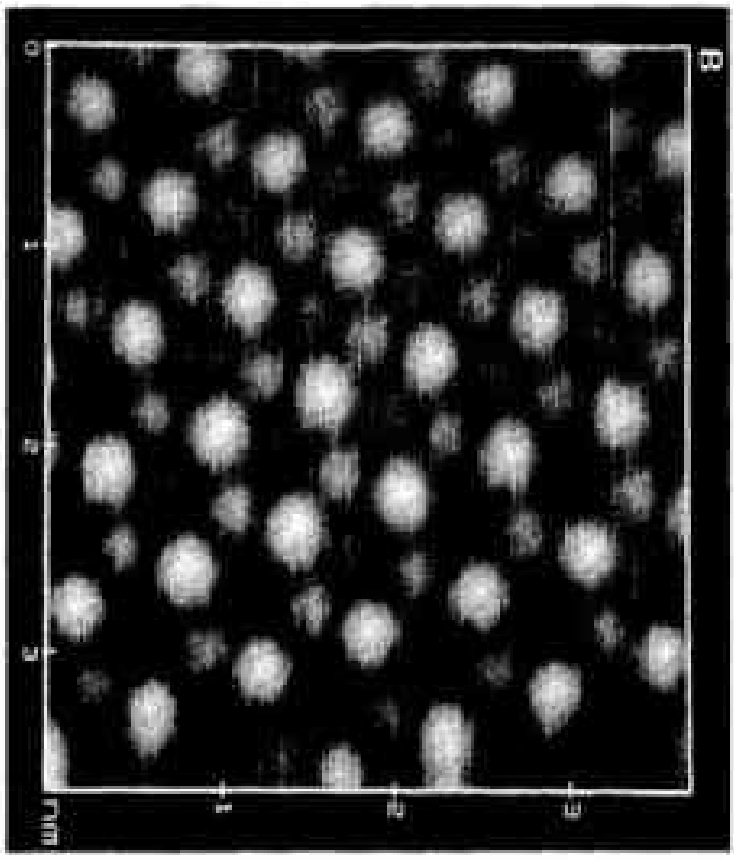

B.C. Schardt, S. L. Yau, F. Rinaldi, ***Science*** 243, 1050 (1989).

N. Batina, T. Yamada, K. Itaya, ***Langmuir*** 11, 4568 (1995).

A. Menzel *et al.*, **Phys. Rev. B** 75, 035426 (2007).

Monolayer Structure

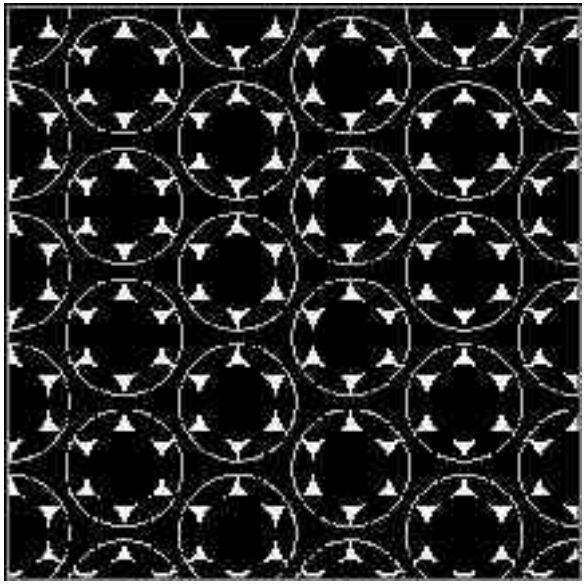

$(\sqrt{3}x\sqrt{3})R30$

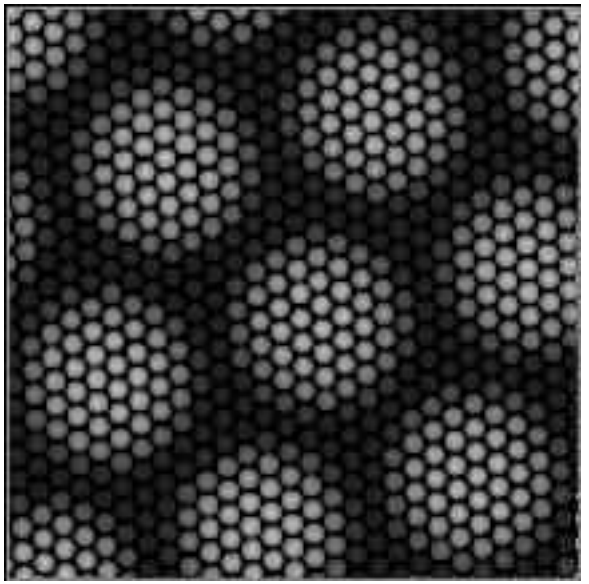

Incommensurate

Striped

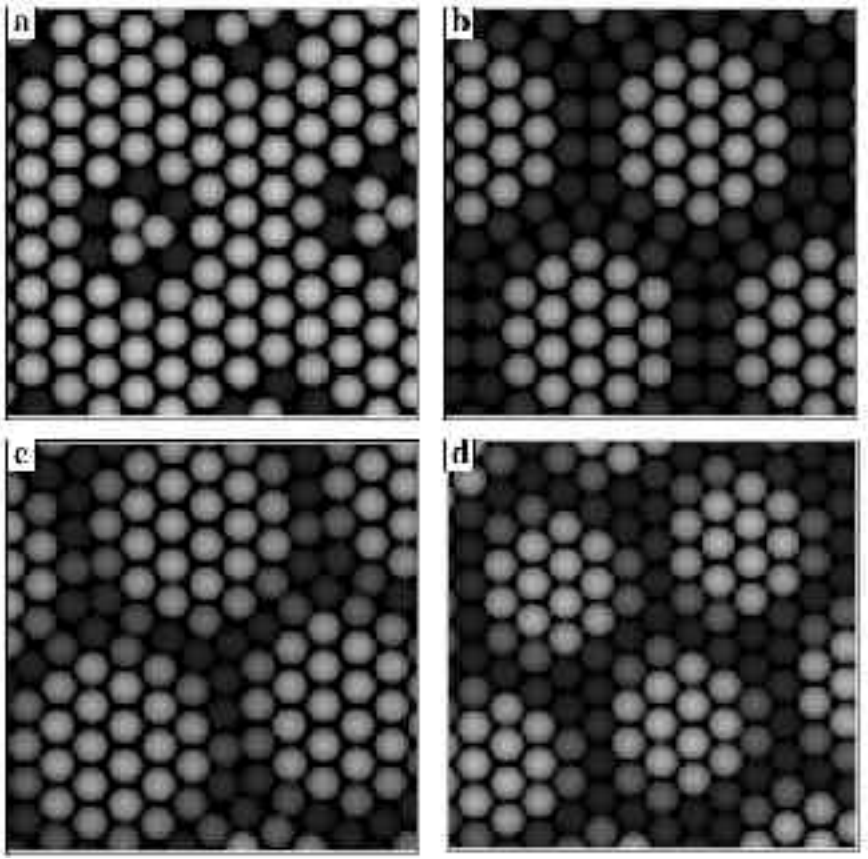

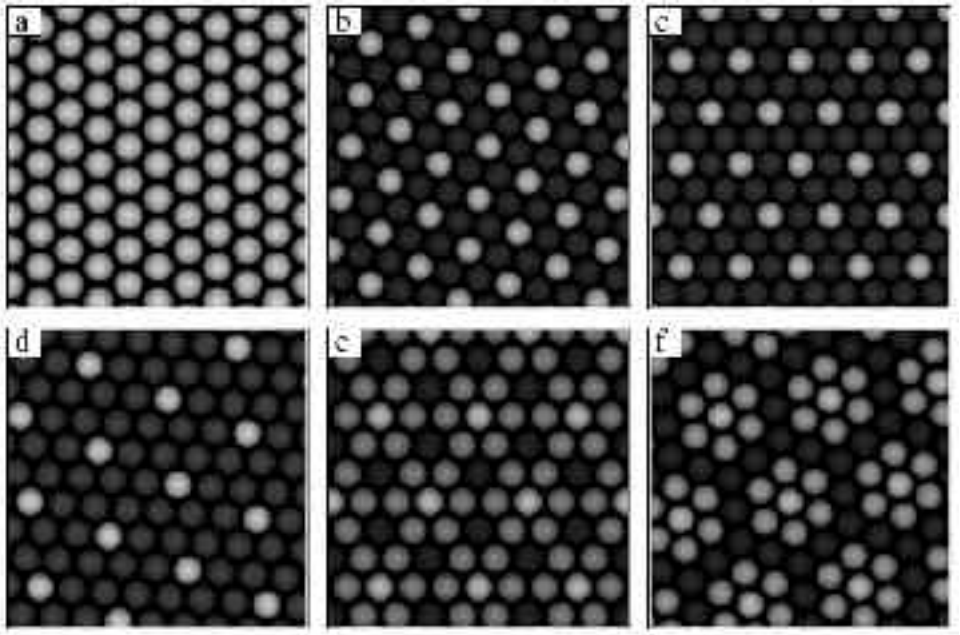

Commensurate

Monolayer—Surface PES

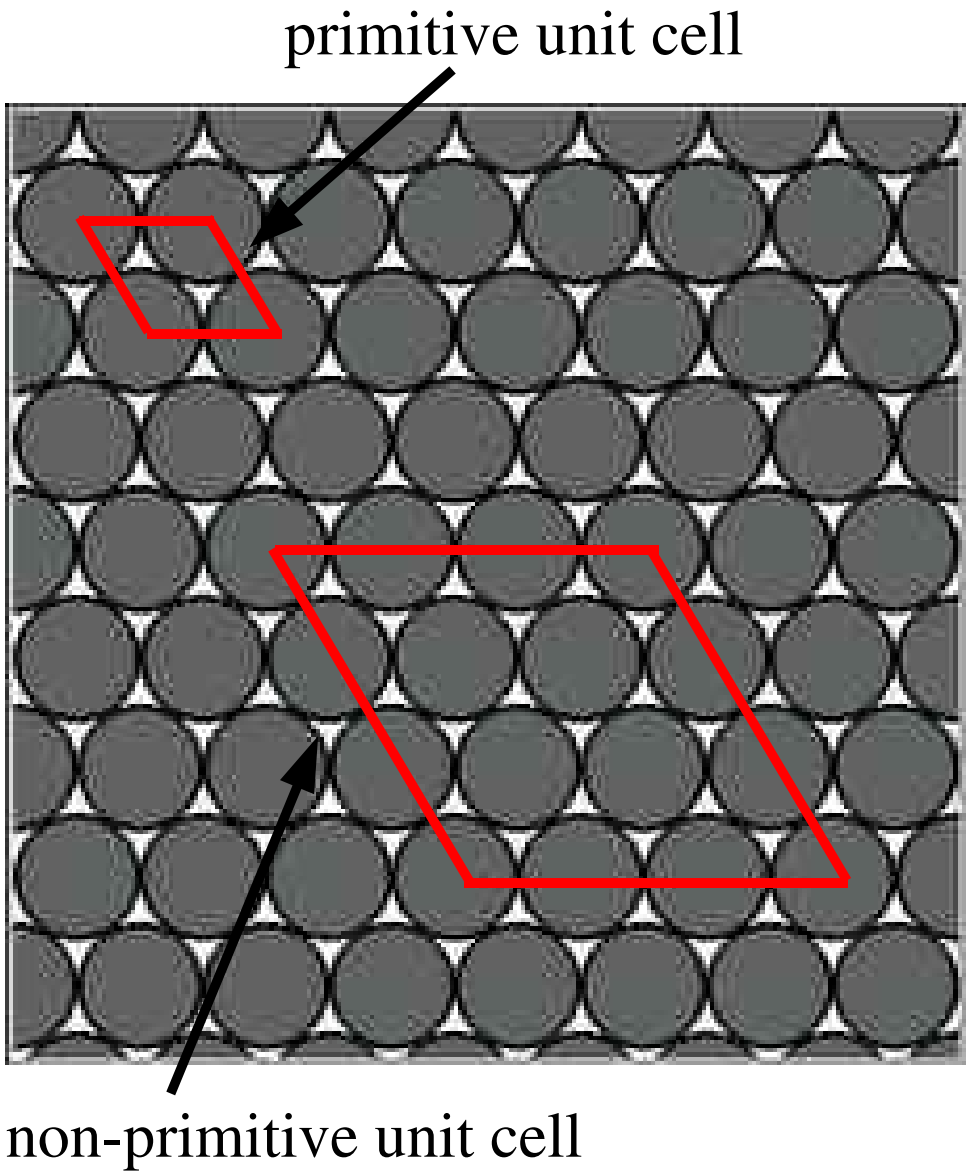

- One is generally interested in the (p,T) phase diagram
- Interestingly, the changes in adsorbate gas (p,T) could be related to the change in ***coverage*** (θ) – the ratio of adsorbate to substrate atoms in the unit cell
- Therefore, one is looking for the lowest energy function $E(\theta)$

Monolayer Epitaxy

Qualitatively different epitaxial behavior, highly system-dependent

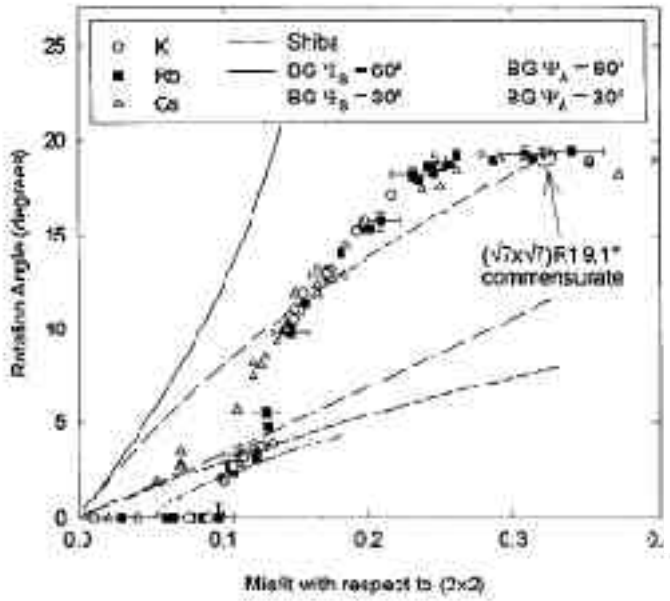

K,Rb,Cs - Ag(111)
(R. Diehl, 1995)

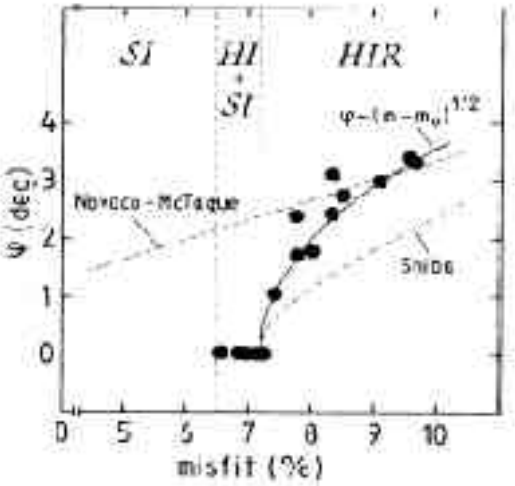

Xe-Pt(111)
(K. Kern, 1987)

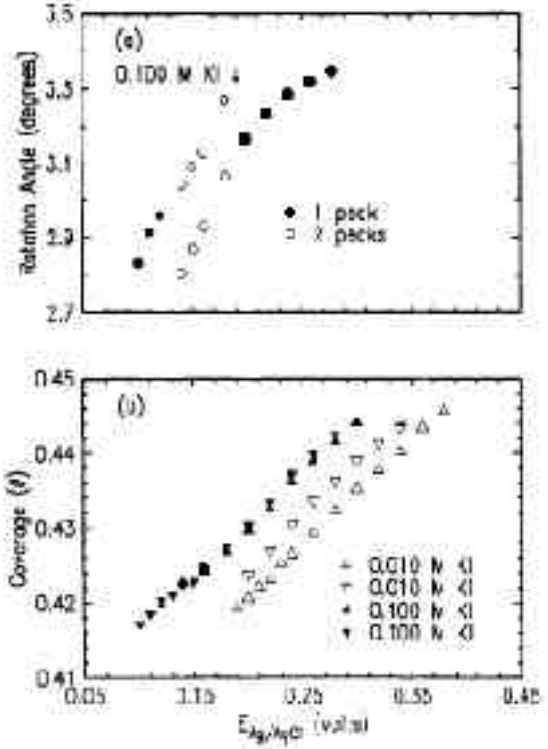

I-Au(111)
(B. Ocko, 1994)

Interaction Potentials

$$E = \sum_{i}^{N} \left(V(x_i, y_i) + \sum_{j>i} F(r_{ij}) \right)$$

$$V(\mathbf{r}) = V_0 + \sum_{G} V_G \exp(-\imath \mathbf{G}\mathbf{r})$$

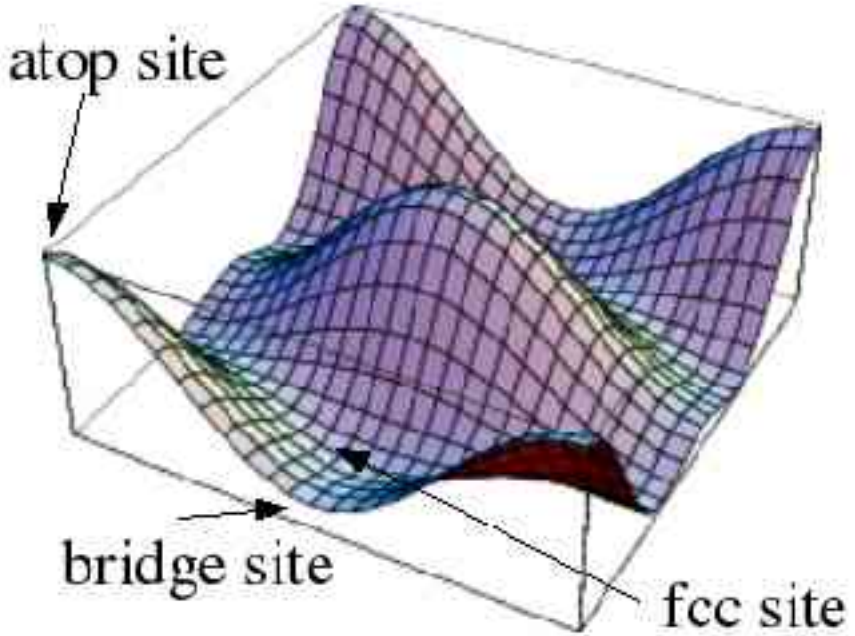

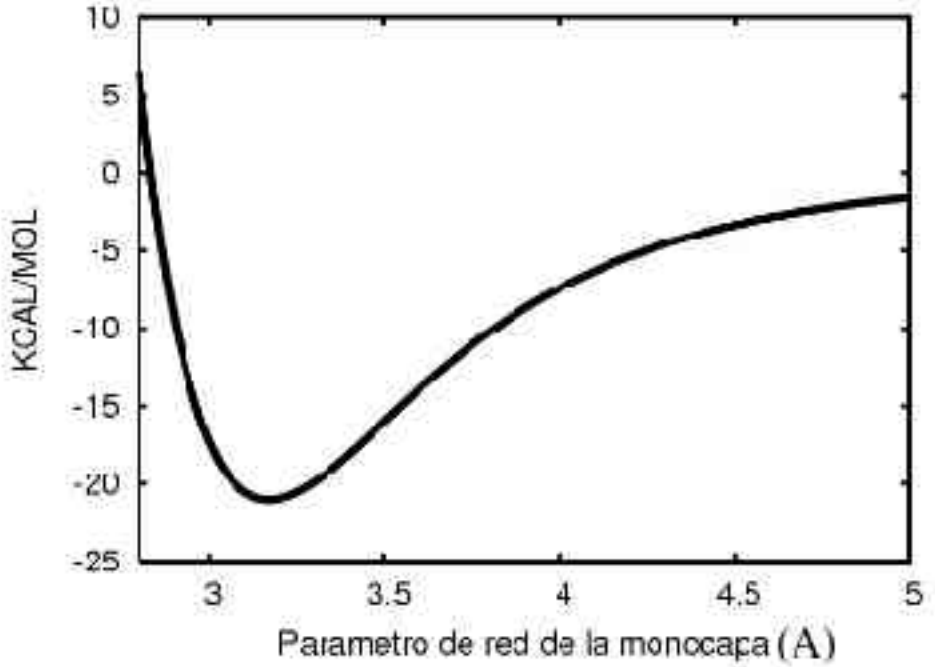

Simple Model Study

- Atom—Surface: Only one Fourier $V(r)$ term
- Monolayer atom-atom: exponential repulsion $Aexp(-Bx)$*

Goals:

1) Cells with $\theta = 1/3$. The global minimum is known exactly !!!

2) How PES changes with the atom—surface potential corrugation and coverage

3) Determination of the lowest energy $E(\theta)$ curve

*A. Tkatchenko, N. Batina, M. Galván, ***Phys. Rev. Lett.*** 97, 036102 (2006).

Simulations

- Generate all possible unit cells with hexagonal symmetry, $N_{ads} < 43$ and $0.33 < \theta < 0.5$
- Periodic boundary conditions in *XY*
- A sufficient number of random quenches from different starting points
- Different algorithms are used for ensuring thorough sampling of the PES

A. Tkatchenko, ***Phys. Rev. B*** 75, 085420 (2007).

PES with Theta = 1/3

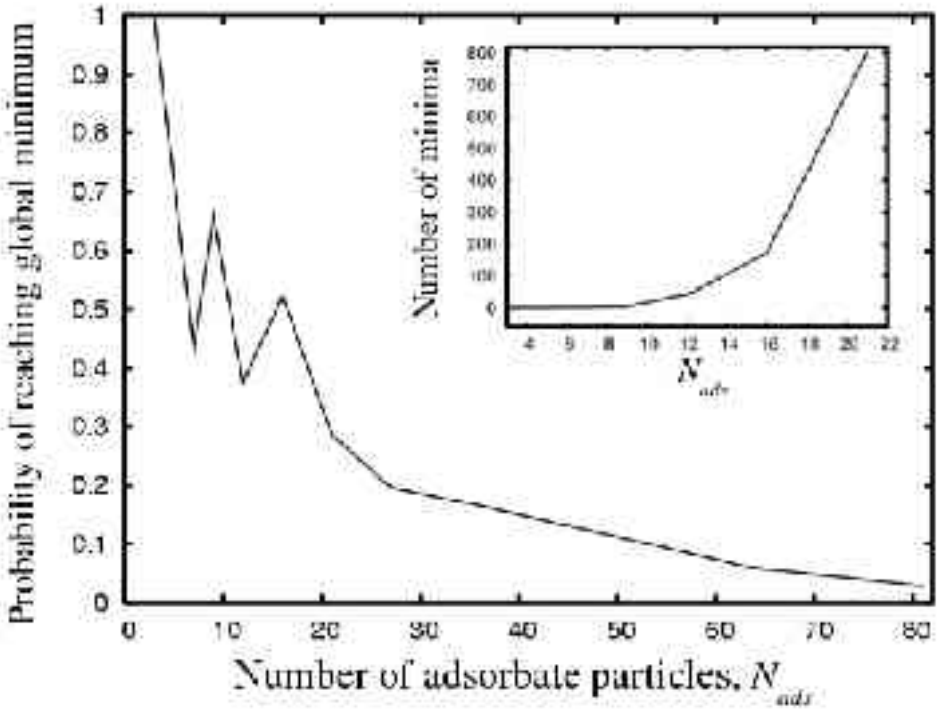

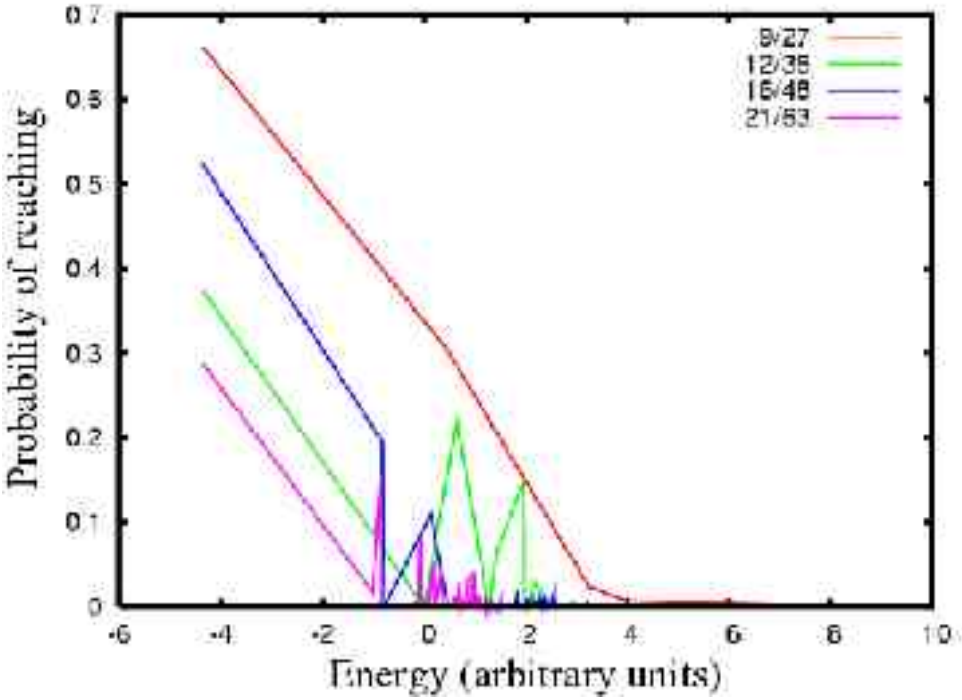

Global minimum →

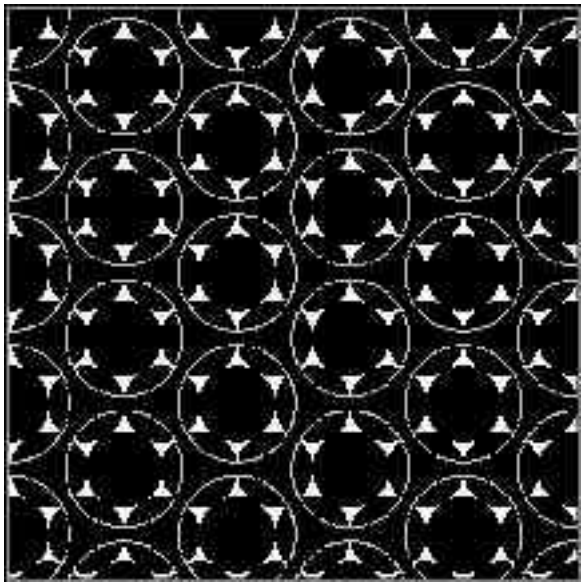

PES of different cells

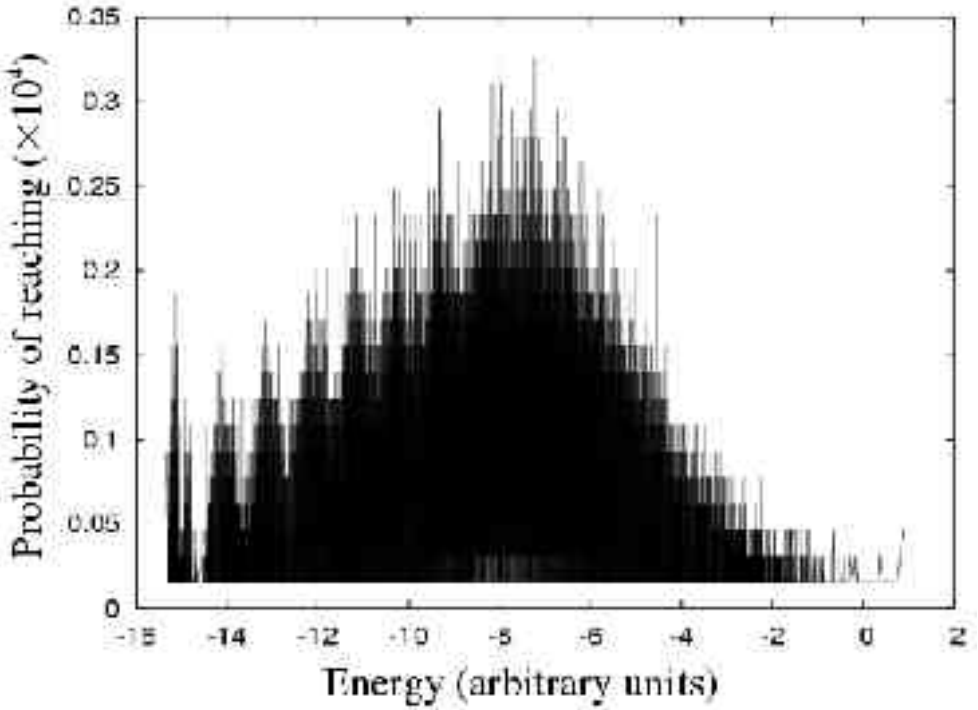

37/112 cell

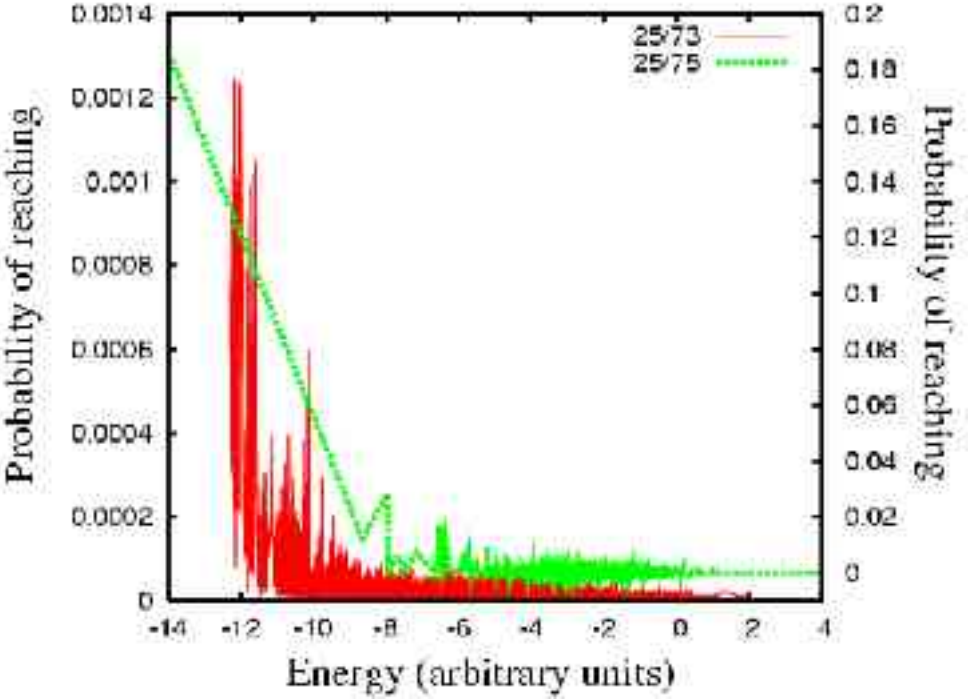

25/75 vs. 25/73

Exhaustive simulations for N_{ads}<43

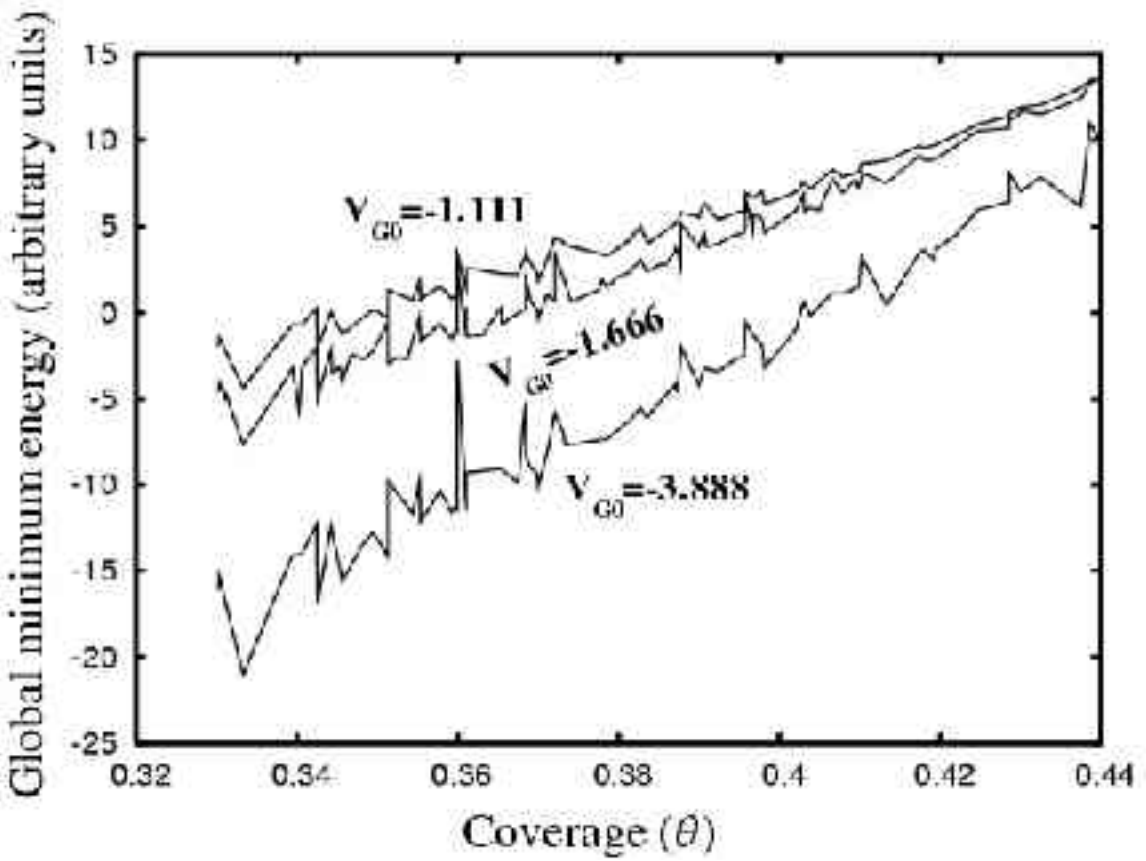

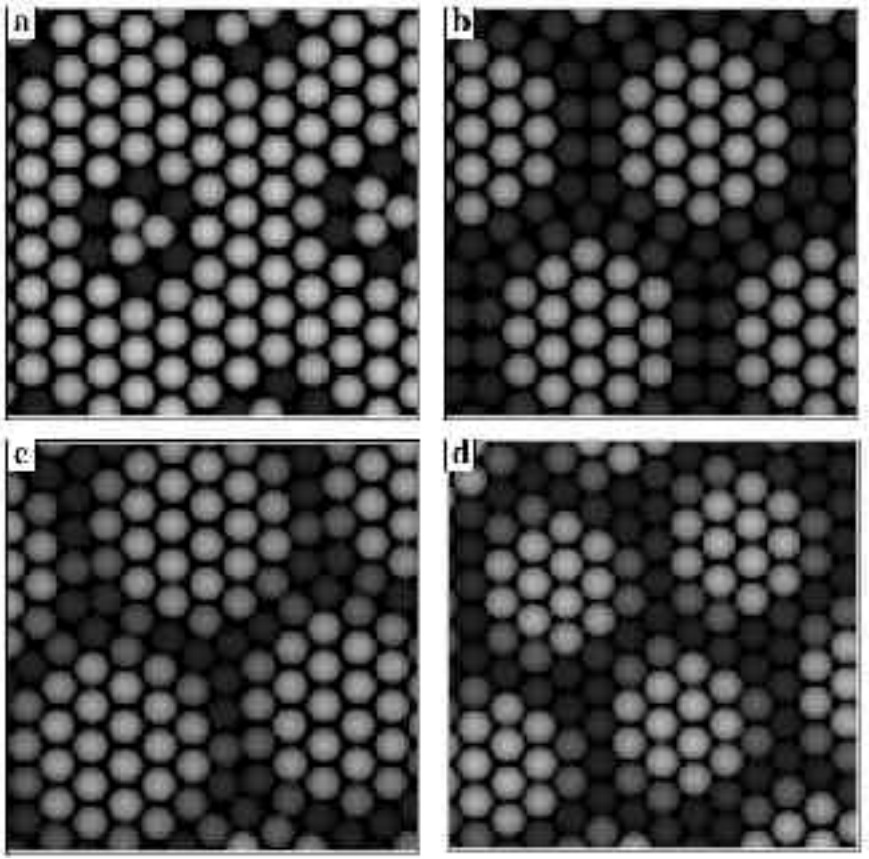

A. Tkatchenko, ***Phys. Rev. B*** 75, 085420 (2007).

PES details

- For $N_{ads} < 43$ and $0.33<\theta<0.5$, the PES most probably consists of a single funnel. However, several cells exhibit complex behavior.
- 1 000 random quenches are sufficient for reaching the global minimum in most cells.
- 50 000 random quenches are needed for at least 3 cells.

Potential Effect

- Higher atom—atom repulsion effectively reduces the complexity of the PES (less local minima)
- The increase in the atom—surface potential corrugation has an opposite effect, allowing atoms to move more freely on the surface

What about real systems ?

- Rare-gases on metal surfaces are good benchmark systems. In this work, we analyze the Xe-Pt(111) system, thoroughly studied before.

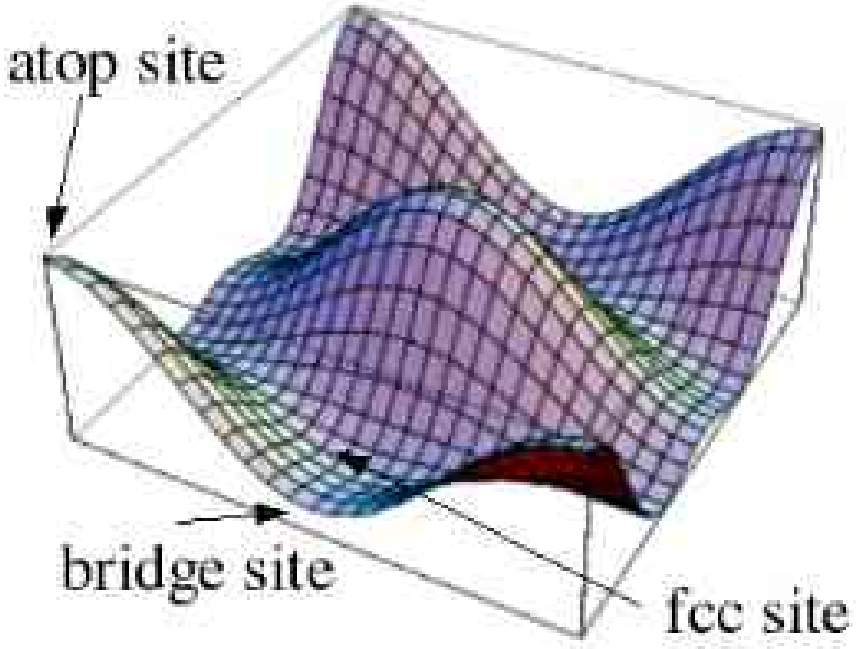

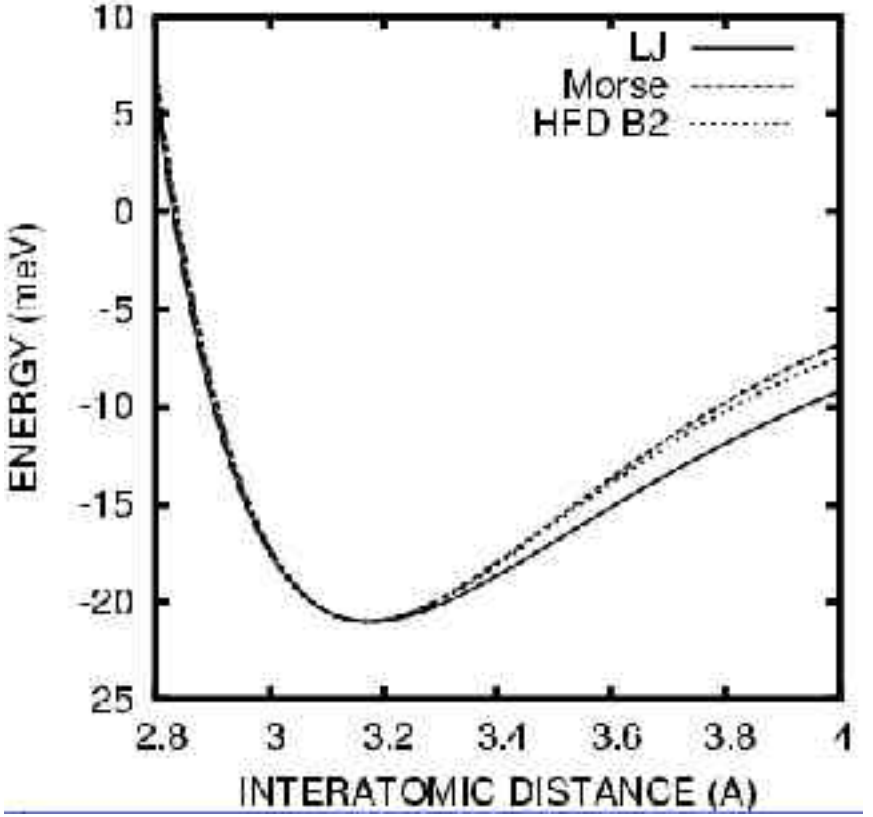

Simulations

- We generate all possible hexagonal unit cells with $N_{ads} < 200$ and $0.33<\theta<0.44$
- Basin-hopping for finding global minima
- Basin-sampling for basin size determination

Basin-hopping simulations

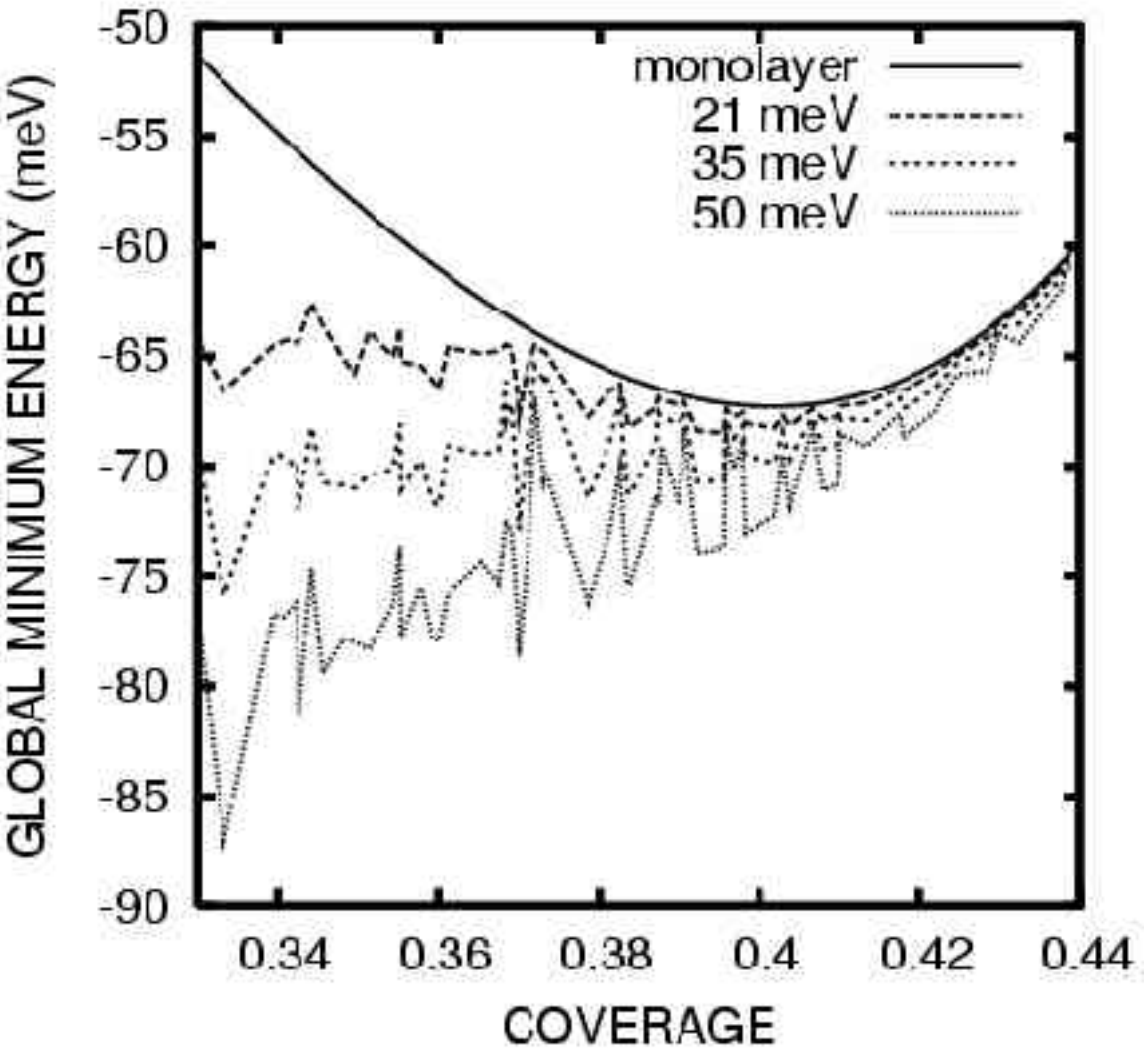

Stable Structures: New Epitaxy ?

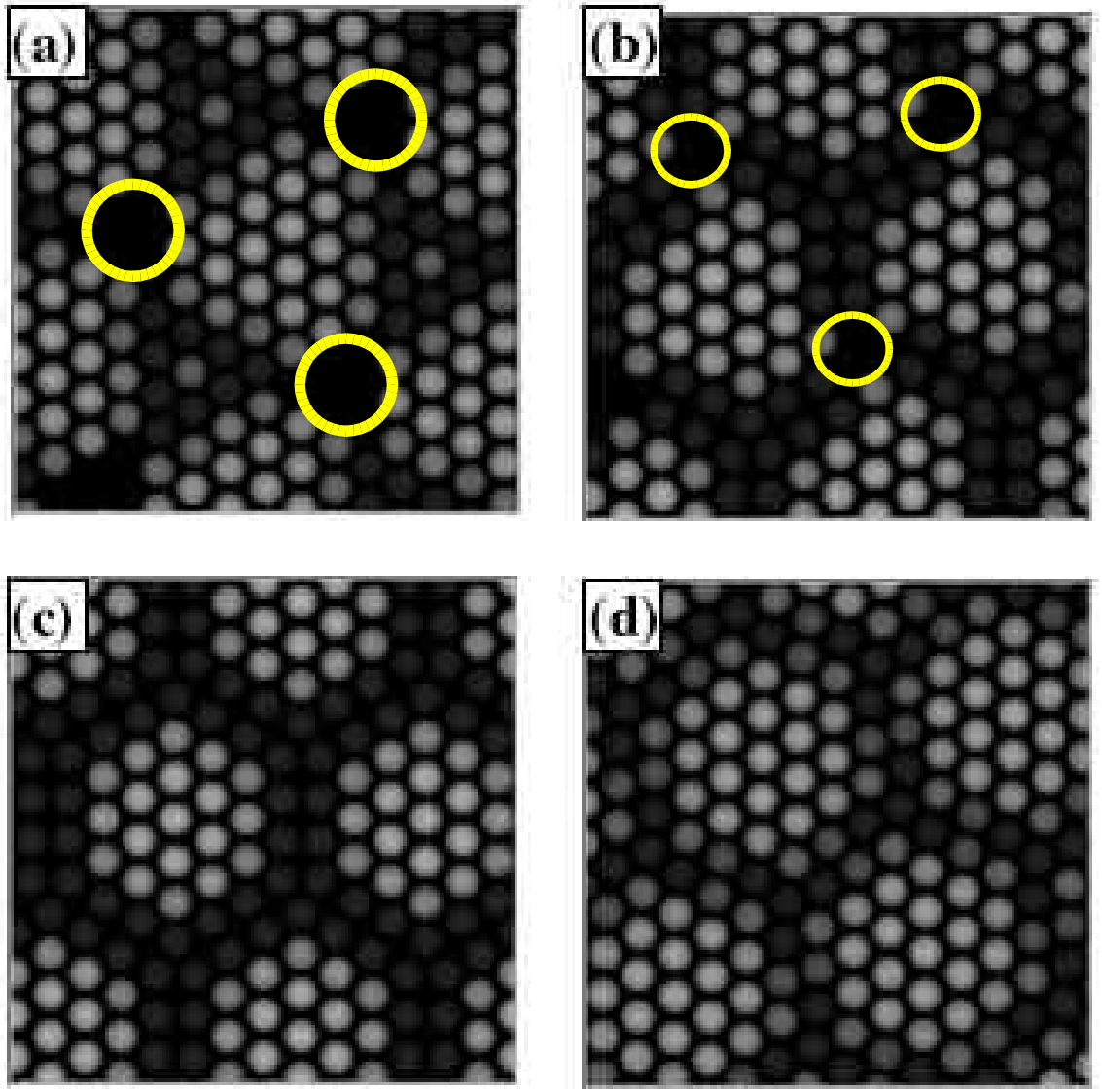

Experimentally, a C-->SI-->HI-->HIR structure sequence is obtained.

We find C-->SI+SIH-->HIR structure sequence.

Potential Range Effect

- The range of the potential increases Morse < HFD-B2 < LJ
- Longer potential range decreases the effective hole size
- The rationale for stability of hole structures is the attractive lateral interaction. This is supported by the fact that they are stable for any value of V_G

PES details

- For $N_{ads} < 65$ and $0.33<\theta<0.44$, the PES consists of a single or double funnel in some cases
- For large N_{ads}, the PES becomes multi-funnel, with a large number of funnels for $N_{ads}=156$
- The longer range of the potential smoothes the PES, as shown before for clusters, etc. The basin-hopping simulations for LJ converge much faster

Finite size effects ?

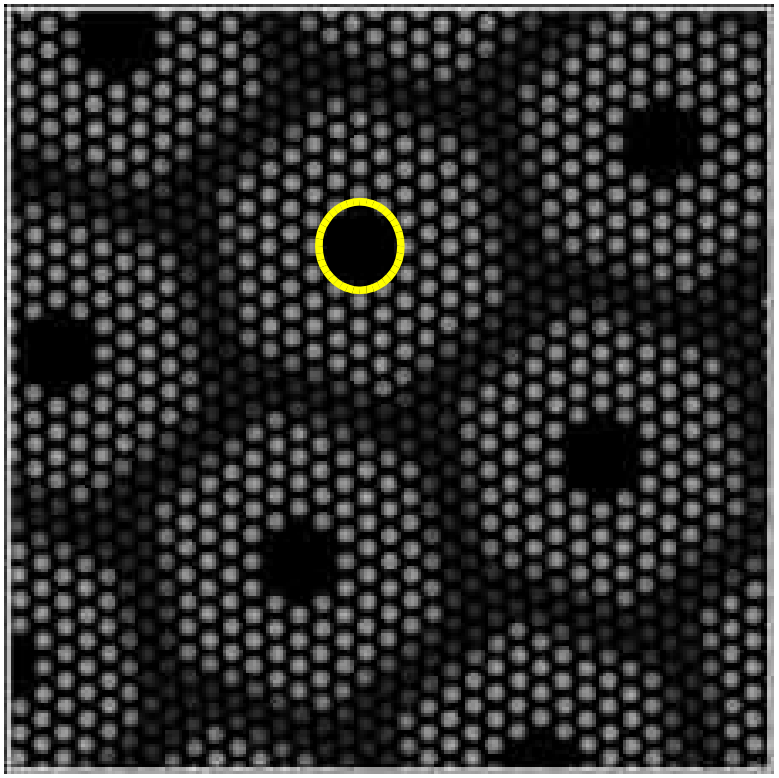

- Hole structures are still stable for N_{ads}=156
- Not yet clear how to “prove” their stability over other type of structures for an infinite monolayer
- The simulations are very computationally intensive, due to PBC

Hole structures: kinetically hindered

- Basin-hopping runs converge mainly to the experimentally found SI or HIR structures without holes, which are higher in energy than SIH ot HIRH
- Basin-sampling runs give the same information: the basin size of the hole structures is too small
- I predict the hole structures appearance to be kinetically hindered

Future Directions

- Obtain disconnectivity graphs for different cells (integrate the potentials into GMIN or OPTIM ?)
- Think how to "prove" the stability of hole structures for infinite monolayer case
- Monolayer phase transitions: Discrete Path Sampling ?
- Investigate the effect of the interaction potentials on monolayer structures in more detail

Acknowledgments

- Marcelo Galván - UAM/Mexico
- Nikola Batina – UAM/Mexico
- CONACYT and LUFAC Computación for financial support
- LUFAC Computación for computer time

QUESTIONS ?

... And on a totally different note:
dispersion-corrected DFT

Summary

- Most used *XC* functionals in DFT have wrong asymptotic behavior --> No dispersion included
- MP2 overbinds
- One must go to CC-CBS to obtain good agreement for systems where dispersion is important: biomolecules, molecular crystals, physisorption, etc.
- However, CC-CBS is only feasible for a few atom systems

DFT + dispersion

- We want to use DFT – low cost first-principles method
- DFT + empirical C_6/R^6 corrections: Grimme, Bechstedt, etc.: works for systems where dispersion is similar to the fitted ones
- Specific long-range *XC* functionals, i.e. Langreth-Lundqvist: seamless dispersion integration, but several approximations involved. Supposed to work better with exact exchange, but not tested yet.

DCACP

- Dispersion Calibrated Atom-Centered Potentials*
- Exactly the same computational cost as pure DFT, so far done for up to 240 atoms
- A pseudopotential is generated for each type of atom, fitted to high-quality CC or MP2 calculation
- The method is transferable, i.e. a Carbon PP fitted to benzene dimer has been shown to be accurate for graphite, fullerene dimer&crystal, interaction between large hydrocarbon molecules, etc.

O. A. von Lilienfeld *et al.*, ***PRL*** 93, 153004 (2004); ***PRB*** 71, 195119 (2005); ***PRB***, submitted (2007).

Examples

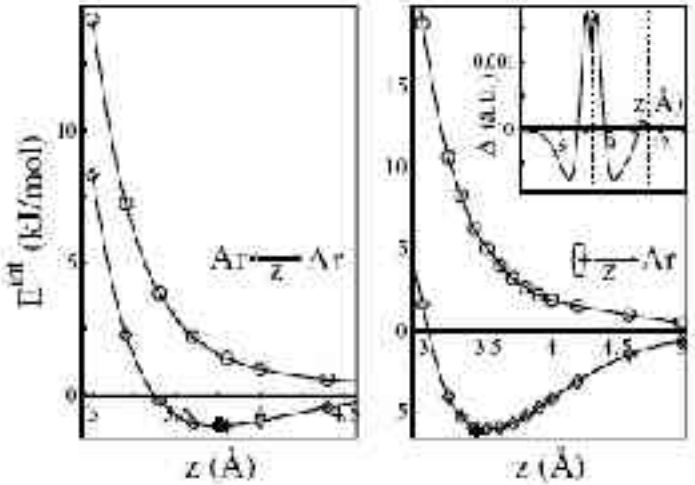

FIG. 2. For the argon-argon and the benzene-argon dimer potential energy curves of the total energy of interaction ($E^{\text{int}} = E^{\text{Dimer}} - 2E^{\text{Monomer}}$) are plotted as a function of the distance z. ○ corresponds to the normal ECPs, ◇ to the optimized LCP (OLCP), and the MP2 results [27] for the interlayer distances and energies of interaction are marked by a cross. In atomic units the calibrated values of the additional f channel for argon are $\sigma_1 = -0.0021$ and $\sigma_2 = 2.902$. In the inset of the right hand panel the C_{6v} symmetry axis z is plotted versus $\Delta = \int dxdy[n^{\text{norm}}(\mathbf{r}) - n^{\text{OP}}(\mathbf{r})]$ (the differences between integrated xy planes of the electron density of the benzene-argon dimer at equilibrium distance computed with the normal ECPs and the OECPs, respectively). The dotted lines show the position of the moieties: benzene (the molecular plane is perpendicular to z) is at 7.85 Å on the z axis, and argon is at 11.26 Å.

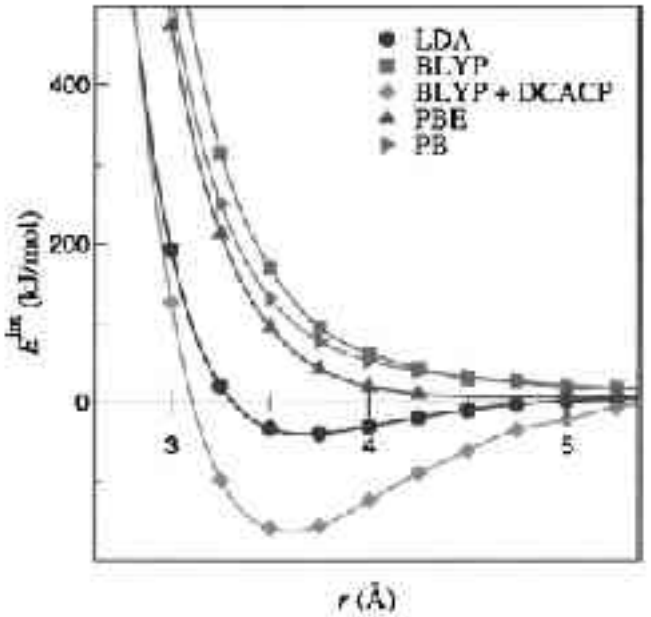

FIG. 2. Total potential energy of interaction for hexabenzocoronene (see structure F, Fig. 1) as a function of intermolecular distance for the LDA, BLYP, PBE, BP, and BLYP–DCACP xc functionals.

O. A. von Lilienfeld, D. Andrienko, ***J. Chem. Phys***. 124, 054307 (2006).

Examples

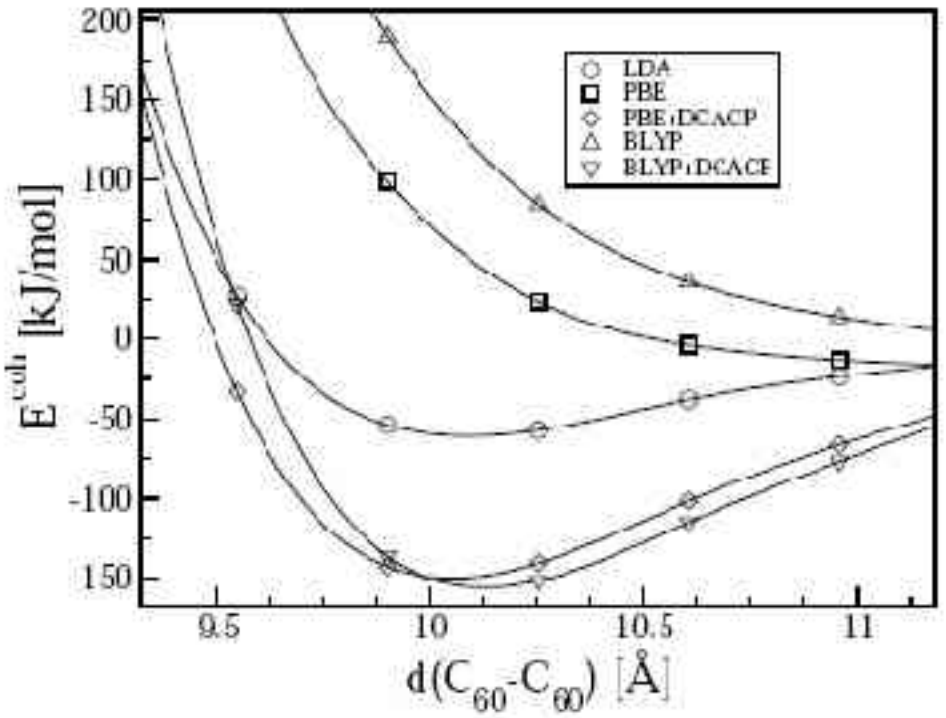

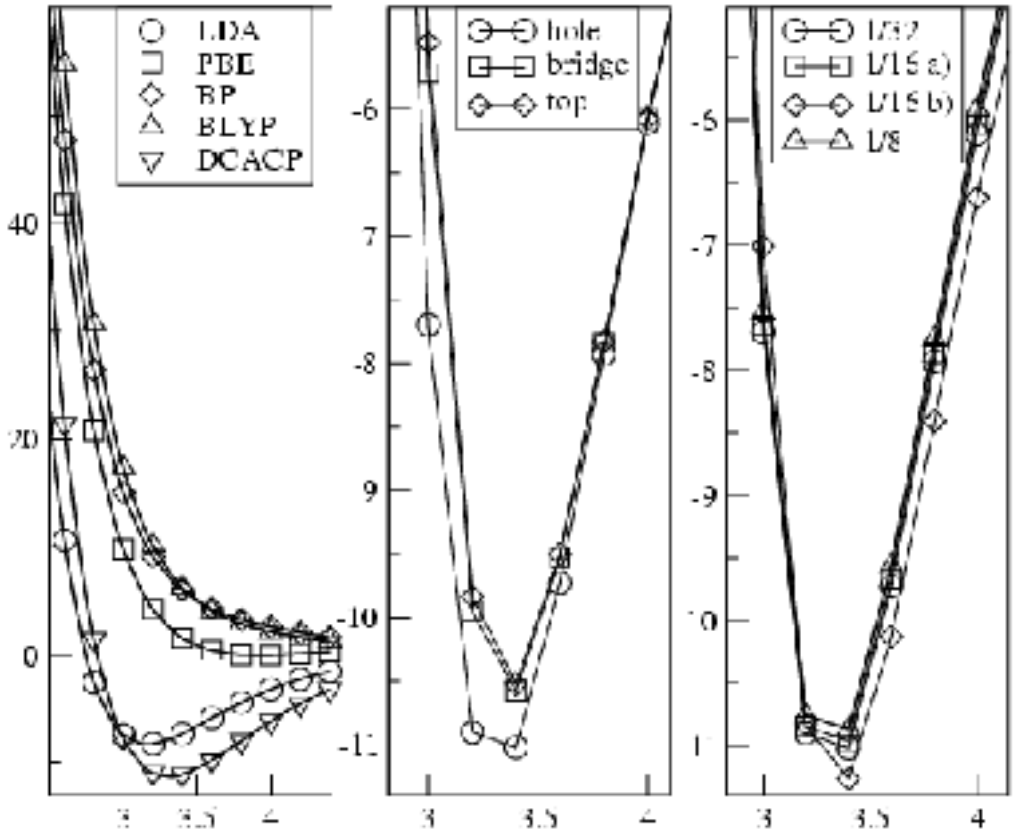

FIG. 3: Γ-point cohesive energy curves vs. lattice constant for the C_{60} crystal using the LDA, PBE, BLYP, BLYP+DCACP, and PBE+DCACP functionals.

- CC-optimed DCACP's give quantitative agreement with experimental data for the cohesive energies of C_{60} dimer and crystal
- The adsorption of Ar on graphite is also in semi-quantitative agreement with empirical models: A. Tkatchenko, O.A. von Lilienfeld, ***PRB*** 73, 153406 (2006).

Conclusions

- DCACP: low-cost seamless method for inclusion of dispersion into DFT
- Transferable to different systems
- Not an ultimate method – but worth giving a try

DCACP's can be downloaded on this page (TM or Goedecker PPs):
http://lcbcpc21.epfl.ch/DCACP/DCACP.html